University of Huddersfield Repository

Muhamedsalih, Hussam, Jiang, Xiang and Gao, F.

Vibration compensation of wavelength scanning interferometer for in-process surface inspection

Original Citation

Muhamedsalih, Hussam, Jiang, Xiang and Gao, F. (2010) Vibration compensation of wavelength scanning interferometer for in-process surface inspection. In: Future Technologies in Computing and Engineering: Proceedings of Computing and Engineering Annual Researchers' Conference 2010: CEARC'10. University of Huddersfield, Huddersfield, pp. 148-153. ISBN 9781862180932

This version is available at http://eprints.hud.ac.uk/id/eprint/9328/

http://eprints.hud.ac.uk/

VIBRATION COMPENSATION OF WAVELENGTH SCANNING INTERFEROMETER FOR IN-PROCESS SURFACE INSPECTION

H. Muhamedsalih, X. Jiang and F.Gao

University of Huddersfield, Queensgate, Huddersfield HD1 3DH, UK

ABSTRACT

A vibration stabilized Wavelength Scanning Interferometer (WSI) is developed for online or in-process measurement purposes. This paper describes the vibration compensation part of the WSI system. The vibration compensation is provided by multiplexing a reference interferometer with the main WSI interferometer. The reference interferometer has a different light source and wavelength from the WSI interferometer but both are sharing common optical path. The reference interferometer serves as a phase-compensating mechanism to eliminate the effects of environmental noise. A structured surface measurement of a semiconductor daughterboard, under mechanical disturbance, is presented. The measurement results showed that the system can withstand environmental noise.

Keywords *Stabilised Interferometer, Wavelength Scanning Interferometer, Piezoelectric Tranducer*

1 THE STABILISED WSI SYSTEM

The optical configuration of the stabilized interferometer is based on multiplexing of two interferometers sharing a common optical path as shown in figure 1. One of the interferometers operates at range of scanning wavelengths from (682.8nm to 529.8nm), known as Wavelength Scanning Interferometer (WSI). The second interferometer has a different light source and known as reference interferometer. The light source of the reference interferometer is a Super Luminescent Light Emitting Diode (SLED)) and operates at wavelength equal to 830nm. The WSI interferometer is used to measure the surface structure as reported by Muhamedsalih et al (2009) and the reference interferometer is used as a feedback source for a close loop control system in order to stabilise the entire interferometry. The stabilised part is a modified version of an original design by Matrin et al (2007) for Phase-Shift interferometry. The two beams paths of the interferometers are combined by a Dichroic mirror DM1 to induce a common beams path and transferred into an optical fiber through a collecting lens L1. The beams are emerged into a Linnik interferometer through a collimated lens L2. The output beams path of the Linnik interferometer are separated by Dichroic mirror DM2. The WSI interferometer output is detected by two dimensional CCD arrays, while the reference interferometer output is detected by Silicon PIN detector.

2 MATHEMATICAL MODELING OF SERVO CONTROL SYSTEM

The section derives a mathematical model of a stabilised interferometer control system and describes it as a block diagram. The block diagram is composed of a set point R(s), proportional-integral (PI) controller, piezo-electric traducer, environmental disturbance D(s) and interferometer. The output of the reference interferometer can be used to measure the fluctuations in the optical path length due to environmental disturbance. These fluctuations can be compensated by altering the path length in one of the arms by using a piezo-electric transducer (PZT). The PZT is derived by a close loop control, hence close loop control can lock the PZT to track any alter in the interferometer's path length to eliminate the environmental disturbance affects.

The following is a transfer function derivation of a PZT, starts with a force that can be produced by a piezoelectric in terms of piezo stress T_3 and piezo cross-sectional area A,

$$F = -T_3 A \qquad \qquad \text{...(1)}$$

The fundamental piezoelectric equation below, of longitudinal vibration mode, describes the piezoelectric element's strain S_3 in terms of material properties (Modulus of elasticity c_{33}^E, Piezo-electric strain coefficient d_{33}) and the stress that caused by the electric field E (Lin W et al (1992)).

$$S_3 = c_{33}^{E} T_3 + d_{33} E_3 \qquad \qquad \text{...(2)}$$

Then $T_3 = \dfrac{S_3 - d_{33}E_3}{c_{33}^E}$ ...(3)

By substituting equation 3 into 1, Equation 4 can be obtained:

$F = \dfrac{A}{c_{33}^E}(d_{33}E_3 - S_3)$ ...(4)

In order to find piezoelectric equation that is function of the deformation that caused by a supplied electric field (i.e. the produced displacement x), Newton's second law (F=M*a) can be employed into equation 4. Since piezo acceleration can be represented as d2x/dt2, then

$M * \dfrac{d^2 x}{dt^2} = \dfrac{A}{c_{33}^E}(d_{33}E_3 - S_3)$ ...(5)

The strain S_3 can be replaced by (x/l). And by adding the damping effect, the piezoelectric equation can be rewritten as:

$M\dfrac{d^2 x}{dt^2} + \beta\dfrac{dx}{dt} + \dfrac{A}{c_{33}^E l}x = (\dfrac{Ad_{33}}{c_{33}^E})E_3$ ...(6)

where β represents the damping coefficient.

Equation 6 shows that the oscillation of the mass is sustained by the piezoelectric force, which is generated by the applied electric field:

$F = (\dfrac{Ad_{33}}{c_{33}^E})E_3$

The Laplace of equation 6 is shown below:

$M s^2 X + \beta s X + (\dfrac{A}{c_{33}^E l})X = \dfrac{Ad_{33}}{c_{33}^E}E$ ...(7)

Then the transfer function of piezoelectric equation is shown in equation 8.

$G_2(s) = \dfrac{X(s)}{E(s)} = \dfrac{\dfrac{A}{M c_{33}^E}d_{33}}{s^2 + \dfrac{\beta}{M}s + \dfrac{A}{M c_{33}^E l}}$ ...(8)

The block diagram of the close loop stabilized interferometer can be represented as shown in figure 2 by considering a PI controller with a transfer function $K_p(1+1/T_i s)$. Furthermore, by setting the photodetector of the interferometer at the maximum intensity of a fringe, and assuming the vibration displacement is not exceeding half of the wavelength (i.e.≈400nm), then the generated interferometer signal voltage is related proportional to the input displacement. Hence the interferometer transfer function can be described as a gain K_{interf}. The integral time and gain of the controller has been set equal to 0.29msec and 1.5 respectively. The PZT model that was used is P-249.10 from (Physik Instrumente, Karlsruhe-Germany).

3   RESULTS AND DISCUSSION

The effectiveness of the servo control system was investigated by carrying out the following experiments. First, a semiconductor daughterboard sample was measured without inducing mechanical disturbance as shown in Figure 3(a). One profile of the sample is shown in Figure 3(b) and illustrates the surface step with height 4.7564μm. Next, a 40Hz and 400nm peak-to-peak sinusoidal mechanical disturbance using a PZT was applied to the reference mirror using a PZT. During the disturbance, the sample was measured as shown in Figure 4. Figure 4(a) shows that the measured signals are distorted by the mechanical vibration signal, although the step height of the sample can still be recognized. One profile of the sample is shown in Figure 4(b) and illustrates the surface step with height 11.711μm. However, the surface roughness signal is completely distorted. When the

vibration compensation is switched on, a reduction in the disturbance movement of the fringe pattern is clearly observed. The measurement of the sample at this stage is carried out; see Figure 5. Figure 5(a) shows that the data were retrieved as the original measurement and illustrates that the compensation vibration can be used to overcome environmental disturbance. One profile of the sample cross-sectional plot in Figure 5(b) shows that the step height is 4.7429µm. The difference between the two measured step height values is 13.5nm in comparison with the two measured results as shown in Figures 3(b) and 5(b). The observed disturbance attenuation between the second and the third parts of the experiment was 12.8dB according to the reference interferometer signal output as shown in Figure 6, which is in agreement with the measured sample error.

The experiments were repeated at different frequencies and the attenuation of the disturbance was recorded as shown in figure 7. The reduce effectiveness of the vibration compensation at higher frequencies could be due to the limit of operating frequency of the piezo system.

4   CONCLUSION

An 850nm wavelength SLED sharing the same optical path of the measurement interferometer can be used to introduce a feedback loop for vibration compensation. The servo system can track and compensate vibration displacements of up to half of the light source wavelength (i.e. 405nm for the proposed system). The results show that disturbance was reduced by 12.8 dB at a vibration frequency of 40Hz. The attenuation of the disturbance is reduced gradually by increasing the applied frequency to reach 6.8dB at 300Hz.
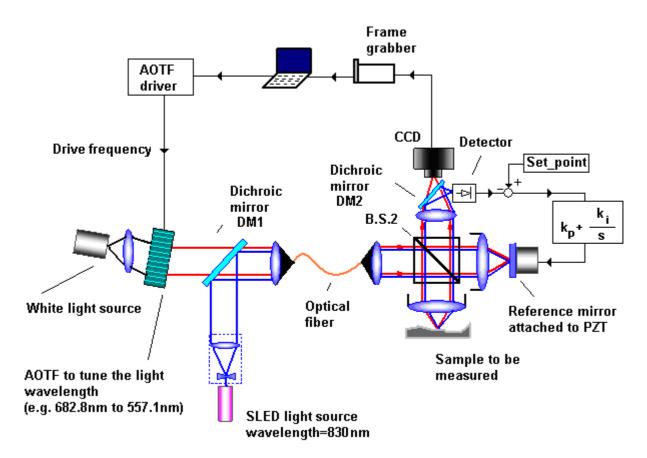
REFERENCES

LIN W and et al, (1992), *The Transfer Function of the Thin Shell PZT Ceramic Cylinder as a Phase Modulator in Fiber Optics Sensors*, Optical Sensors, SPIE Vol.1814.

MARTIN H., WANG K. and JIANG X. (2007), *Vibration Compensation Beam Scanning Interferometer for Surface Measurement*, Applied Optics, Vol.47, No. 7.

MUHAMEDSALIH H., JIANG X. and GAO F. (2009), *Interferograms Analysis for Wavelength Scanning Interferometer Using Convolution and Fourier-Transform*, University of Huddersfield, ISBN:978-1-86218-067-3, p33-37.

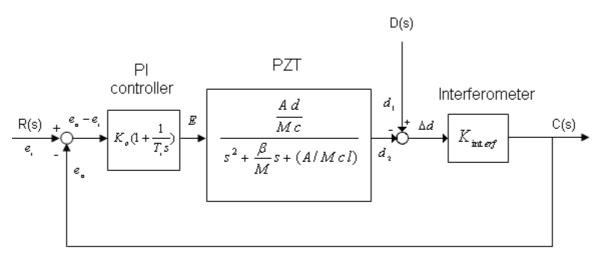UCHINO K., and GINIEWICZ J, (2003) Micromechatronics, Marcel Dekker Inc.

Figure 1: Configuration of the proposed vibration stabilized Interferometry

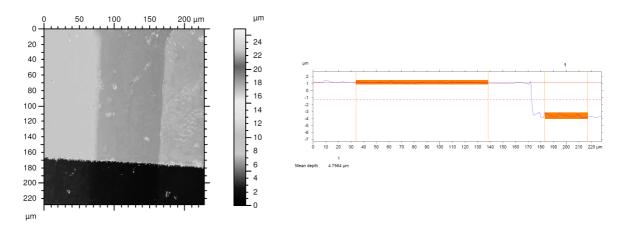**Figure 2: Block diagram of the stabilized Interferometer control loop**

Figure 3: Measurement results of a semiconductor daughterboard sample without an induced mechanical disturbance. (a) The measured surface; (b) A cross-section profile
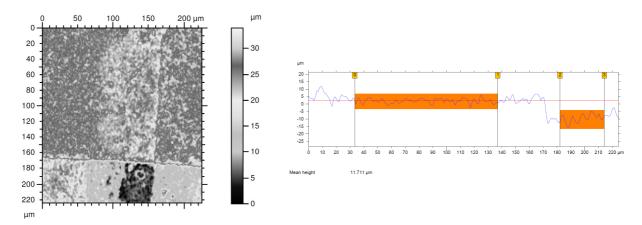

Figure 4: Measurement results of a semiconductor daughterboard sample with a sinusoidal mechanical disturbance of 40 Hz. (a) The measured surface; (b) A cross-section profile
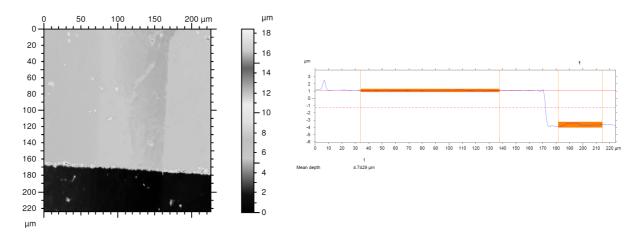

Figure 5: Measurement results of a semiconductor daughterboard sample with the vibration compensation. (a) The measured surface; (b) A cross-section profile
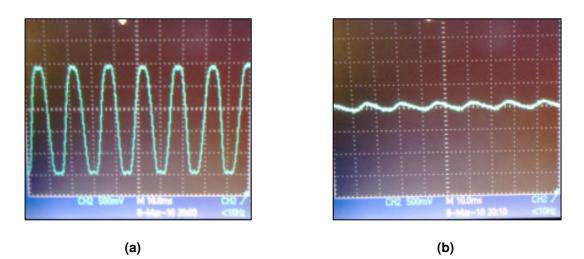
(a)　　　　　　　　　　　　　　　　　　　**(b)**

Figure 6: Effect of vibration compensation on a 40 Hz and 400 nm peak to peak sinusoidal disturbances. (a) Before stabilization; (b) after stabilization
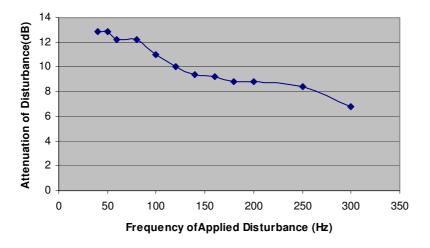

Figure 7: Attenuation of 400nm peak to peak applied disturbance